Neuron, Vol. 20, 783–795, April, 1998, Copyright ©1998 by Cell Press

Spillover-Mediated Transmission at Inhibitory Synapses Promoted by High Affinity α_6 Subunit $GABA_A$ Receptors and Glomerular Geometry

David J. Rossi* and Martine Hamann
Department of Physiology
University College London
London WC1E 6BT
United Kingdom

Summary

Divergence and convergence of synaptic connections make a crucial contribution to the information processing capacity of the brain. Until recently, it was thought that transmitter released at a synapse affected only a specific postsynaptic cell. We show here that spillover of inhibitory transmitter at the Golgi to granule cell synapse produces significant cross-talk to non-postsynaptic cells, which is promoted both by the anatomical specialization of this glomerular synapse and by the presence of the high affinity α_6 subunit-containing $GABA_A$ receptor in granule cells. Cross-talk is manifested as a novel slow rising and decaying small amplitude inhibitory postsynaptic current (IPSC) that can also contribute a long-lasting component to more typical IPSCs, which is prolonged by inhibition of the neuronal GABA transporter GAT-1. Because of the long duration of IPSCs generated by spillover, the total charge carried is three times that of IPSCs generated by directly connected terminals. GABA spillover within the mossy fiber glomerulus may play an important role in regulating the number of granule cells active in the cerebellar cortex, a regulation that is suggested by theoretical models to optimize cerebellar information processing.

Introduction

It has been a dogma in our understanding of neuronal information processing that the "fast" neurotransmitters—glutamate, acetylcholine, GABA, and glycine—mediate communication between neurons only at specific synaptic sites. Transmitter action is thought to be localized spatially by geometrical factors or by uptake of transmitter into neurons or glial cells (Isaacson et al., 1993; Barbour et al., 1994; Clements, 1996; Asztely et al., 1997; Takahashi et al., 1997). Recently, however, it has been suggested that glutamate released from one presynaptic neuron can spill over and activate receptors that are anatomically postsynaptic to a different presynaptic neuron or that occupy extrasynaptic locations on the postsynaptic neuron (Kullmann et al., 1996; Barbour and Häusser, 1997; Asztely et al., 1997). Receptor activation by the relatively low transmitter concentration produced by spillover is particularly likely to occur when the receptors have a high affinity for the transmitter, as is the case for NMDA receptors at glutamatergic synapses. Spillover of transmitter introduces a divergence of information flow superimposed on that produced by divergence in the wiring of synaptic connections. In the case of glutamate, it may also have significant implications for our understanding of the mechanisms of synaptic plasticity (Kullmann et al., 1996; Malenka and Nicoll, 1997).

Although a modulation of excitatory transmission by GABA spillover has been observed in the hippocampus (Isaacson et al., 1993), little is known about whether spillover-mediated transmission occurs at inhibitory synapses. We therefore studied inhibitory transmission at a synapse that seems anatomically specialized to promote spillover: the Golgi cell to granule cell synapse in the cerebellar cortex (Figures 1A and 1B), which has been suggested to play a key role in regulating information processing by the cerebellum (Marr, 1969). This synapse is localized within a glomerulus (Hámori and Szentágothai, 1966; Jakab and Hámori, 1988; Jakab, 1989). Each glomerulus is centered on the large, axonal terminal of a glutamatergic mossy fiber afferent. The mossy fiber terminal is surrounded by granule cell dendrites that arise from 50–60 distinct granule cells, each of which sends a single dendrite to each glomerulus. Intermingled with, but somewhat more peripheral to, this granule cell dendrite corona are numerous Golgi cell axon terminals that form GABAergic synapses with the granule cell dendrites. This mesh of dendritic and axonal processes is wrapped by a glial sheath. GABA released at Golgi to granule cell synapses is probably confined within the glomerulus by the glial sheath, and removed by uptake into Golgi cell terminals and into the glial cell(s) ensheathing the glomerulus (Itouji et al., 1996). Thus, any GABA escaping from the synaptic cleft is likely to encounter GABA receptors on other granule cell dendrites within the glomerulus, especially because GABA receptors are known to be expressed both in postsynaptic and extrasynaptic locations within the glomerulus (Nusser et al., 1995, 1996, 1998). This anatomical constraint, combined with the fact that granule cells are the only cells expressing the α_6 subunit of the $GABA_A$ receptor, which endows receptors with an affinity for GABA that is an order of magnitude higher than the more generally occurring α_1 subunit (Ducic et al., 1995; Saxena et al., 1996), provides a potent basis for spillover-mediated inhibitory cross-talk within the glomerulus. Although spillover has not been directly demonstrated, recent observations of a tonic, TTX-sensitive GABA-mediated current in granule cells were interpreted in terms of GABA accumulation in the glomerulus (Wall and Usowicz, 1996, 1997; Brickley et al., 1996).

Here, we analyze spontaneous and evoked IPSCs at this synapse, show that cross-talk does indeed occur, and investigate the role of GABA transporters in limiting the extent of cross-talk.

Results

Initially, we describe the basic properties of Golgi cell to granule cell transmission, some of which have not been reported previously. We then present a detailed

*To whom correspondence should be addressed.

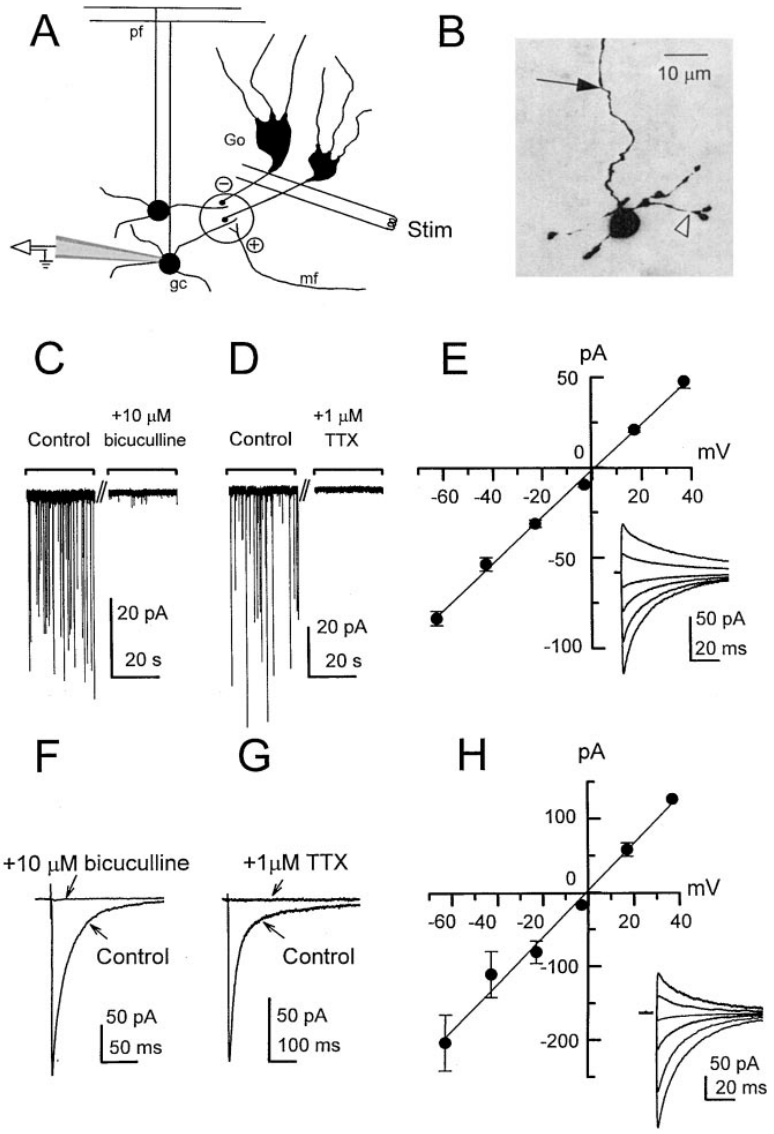

Figure 1. GABAergic Transmission at the Golgi Cell to Granule Cell Synapse

(A) Schematic diagram of the preparation. Patch-clamp recordings were made from granule cells (gc) in 200 μm thick cerebellar slices. Granule cells are innervated by excitatory (+) glutamatergic mossy fibers (mf) and inhibitory (-) GABAergic Golgi cell (Go) axons in the glomerulus (circle). Granule cell axons form the parallel fibers (pf). The stimulating electrode (Stim) was positioned in the granule cell layer close (<150 μm) to the recorded granule cell.

(B) Black and white reversed image of a granule cell filled with Lucifer yellow from the pipette. Arrow points to the ascending axon. Arrowhead points to one of the four dendrites.

(C and D) Continuous recordings illustrating that spontaneous synaptic currents were abolished by 10 μM bicuculline (C) and by 1 μM tetrodotoxin (D).

(E) Mean I-V relationship for the peak spontaneous synaptic current reverses at 1.4 ± 0.9 mV in six cells (E_{Cl^-} = 0.5 mV). The inset shows spontaneous IPSCs from one cell at potentials from −63 mV to 37 mV (20 mV steps), aligned on their rising phase. The 10%–90% decay time was voltage dependent, being 42 ± 2.5 and 75 ± 7.4 ms ($p < 0.05$, n = 6) at −63 and 37 mV, respectively. Values are corrected for the liquid junction potential.

(F and G) Evoked synaptic currents were abolished by 10 μM bicuculline (F) and by 1 μM tetrodotoxin (G).

(H) I-V relationship for the peak evoked IPSC reverses at −0.9 ± 2.7 mV in three cells (E_{Cl^-} = 0.5 mV). The inset shows eIPSCs from one cell at potentials from −63 mV to +37 mV (20 mV steps). The 10%–90% decay time was 61 ± 8.4 and 160 ± 47.7 ms ($p > 0.05$, n = 3) at −63 and 37 mV, respectively. The stimulation artifact was blanked on the eIPSC traces. Values are corrected for the liquid junction potential.

analysis of the kinetics of transmission and demonstrate the importance of GABA spillover.

Properties of Spontaneous Inhibitory Postsynaptic Currents

Recordings made from granule cells in 200 μm cerebellar slices from 12-day-old rats display spontaneous inward currents at a holding potential of −60 mV (Figures 1C and 1D; see also Puia et al., 1994; Kaneda et al., 1995; Brickley et al., 1996; Wall and Usowicz, 1997). These currents occurred at frequencies ranging from 0.02–2.3 Hz (mean = 0.5 ± 0.06 Hz, n = 61). With near equimolar Cl^- inside and outside of the cell (E_{Cl^-} = 0.5 mV), the currents displayed linear current–voltage relations and reversed at 1.4 ± 0.9 mV (n = 6; Figure 1E). The spontaneous inward currents were abolished by the bath application of either 10 μM bicuculline (n = 53; Figure 1C) or 1 μM TTX (n = 8; Figure 1D) and thus represent the spontaneous action potential–dependent release of GABA from Golgi cells onto granule cells. These currents will be referred to as spontaneous inhibitory postsynaptic currents (sIPSCs).

Evoked Inhibitory Postsynaptic Currents

IPSCs could also be evoked by electrical stimulation in the granule cell layer (Figures 1A and 1F–1H). Evoked IPSCs (eIPSCs) had a pharmacology and voltage dependence similar to that of the sIPSCs (Figures 1F–1H); they displayed linear current–voltage relations (Figure 1H), reversed at −0.9 ± 2.7 mV (n = 3), and were abolished by 10 μM bicuculline (n = 45; Figure 1F) or 1 μM TTX (n = 14; Figure 1G).

Kinetic Properties of Evoked and Spontaneous IPSCs

Both sIPSCs and eIPSCs had a rapid rise time (10%–90% rise time = 0.5 ± 0.02 ms, n = 30 cells and 1.4 ± 0.1 ms, n = 20 cells, respectively, $p < 0.05$) and decayed with a time course described by the sum of either two or three exponentials (Table 1). Because it is difficult to compare waveforms fit with the sum of two and of three exponentials, we present comparisons of IPSC decay in different cells in terms of the 10%–90% decay time. The decay of the eIPSC was 2.52-fold slower ($p < 0.05$) than the sIPSC in the same cell (sIPSC 10%–90%

Table 1. Parameters Describing the Decay Phrase of the IPSCs

	τ_1 (ms)	A_1 (pA)	τ_2 (ms)	A_2 (pA)	τ_3 (ms)	A_3 (pA)	A_1 (%)	A_2 (%)	A_3 (%)	n
sIPSCs		−25.9 ± 6.1	12.9 ± 1.3	−59.0 ± 12.2	62.4 ± 6.2	−23.0 ± 4.9		68 ± 5	32 ± 5	18
	3.7 ± 0.4		15.9 ± 1.5	−54.3 ± 8.1	91.8 ± 12.5	−11.1 ± 2.2	27 ± 3	60 ± 2	13 ± 2	12
eIPSCs		−40.4 ± 10.5	29.0 ± 5.6	−70.9 ± 10.7	198.0 ± 29.8	−32.5 ± 7.8		68 ± 4	32 ± 4	18
	5.8 ± 0.9		27.0 ± 2.8	−80.9 ± 26.0	232.5 ± 28.3	−15.4 ± 3.2	31 ± 4	54 ± 5	15 ± 4	8

The fit with a double or triple exponential function was performed using the Simplex iterative fitting technique where τ_n and A_n are the time constant and the amplitude, respectively, of each component (n). The number of exponentials was determined by eye or by choosing fits that differed from the actual peak of the IPSC by less than 3%.

decay = 46.1 ± 4.4 ms; eIPSC, decay = 116 ± 15 ms, n = 19; Figures 2B and 2D). Although the eIPSC amplitude was the same or larger than the sIPSC in every cell (mean values: 138 ± 18.3 and 92 ± 17.9 pA, respectively, n = 19, p = 0.05; Figures 2A and 2C), there was no correlation between the difference in amplitude and difference in decay time in the same cell (r = 0.26; data not shown).

To explore the mechanisms of the difference in decay rate in eIPSCs and sIPSCs, we examined the individual responses underlying the average eIPSC (Figure 3). There appeared to be three types of response to electrical stimulation: (1) fast rising large amplitude responses (Figures 3A and 3Ai) with a 10%–90% rise time of 1.7 ± 0.2 ms, a peak amplitude of 87.0 ± 12.5 pA, and a 10%–90% decay time of 189 ± 25 ms (n = 12 cells); (2) failures (Figure 3Aii); and (3) slow rising, small amplitude responses that decayed very slowly (Figures 3A and 3Aiii), with a 10%–90% rise time of 30.2 ± 9.6 ms, a peak amplitude of 17.3 ± 2.7 pA, and a 10%–90% decay time of 630 ± 74.8 ms (n = 12 cells). Because of the long duration of the slow rising eIPSCs, the total amount of charge carried is three times that of the sIPSC (Figure 3E).

However, even when separated in this fashion, the fast rising, large amplitude evoked events (Figure 3Ai) still decayed more slowly than the sIPSCs (Figure 3B). A simple hypothesis to explain the data is that the evoked postsynaptic currents are comprised of two discrete events, either a slow rising and decaying component on its own (as in Figure 3Aiii), or a fast rising and falling IPSC (as seen occurring spontaneously) superimposed on the slow component (as in Figure 3Ai). Consistent with this hypothesis, mathematical subtraction of the slow rising eIPSC component from the fast rising eIPSC resulted in a waveform with an amplitude (84 ± 7.0 pA), decay time (49.8 ± 10.4 ms), and area (1.8 ± 0.9 pC) similar ($p > 0.05$ for all three values) to those of the sIPSC (n = 4; Figures 3C–3E). While both types of response were blocked by either bicuculline (Figure 1F) or TTX (Figure 1G), neither response was blocked by glutamate or glycine receptor antagonists (data not shown).

The time to half peak of the slow component (as in Figure 3Aiii) was 6.8 ± 2.4 ms (n = 10), which is consistent with diffusion of GABA from a source (equation 1, Experimental Procedures) at a distance comparable with the diameter of a glomerulus (5–6 μm). This suggests that the slow events might reflect activation of $GABA_A$ receptors by spillover of GABA released from nearby, but not directly connected, Golgi axon terminals (For convenience, we refer to such terminals as remote and those making direct synaptic contact with the postsynaptic cell as direct). In the following section, we describe experiments designed to test this hypothesis.

Estimation of the Number of Axon Terminals Underlying the Fast and Slow eIPSCs

If the slow events arise from activation of distinct axons remote from the recorded cell, then the total number of inputs (both direct and remote) capable of being activated during stimulation should exceed the number of axon terminals directly connected to the recorded cell. To examine this possibility, we used stimulus-intensity plots in order to determine the number of terminals underlying the fast and slow rising eIPSCs. Figures 4A and 4B show that the amplitude of the fast component of the eIPSC increased in a stepwise fashion with increasing stimulus strength. Each step represents the recruitment of additional directly connected Golgi axon terminals. By comparing the failure rate of the fast and slow eIPSCs (i.e., the number of occasions on which no fast IPSC or no slow IPSC occurred at all; see Experimental Procedures), we estimate that with minimal stimulation (see Experimental Procedures; Stevens and Wang, 1994) the ratio of remote to direct terminals was 1.2 ± 0.4 (range = 0–4, n = 12). At higher stimulus intensities, this ratio was 1.7 ± 0.6 (range = 0–5.5, n = 10, $p > 0.05$). The estimated ratio of terminal types activated correlated

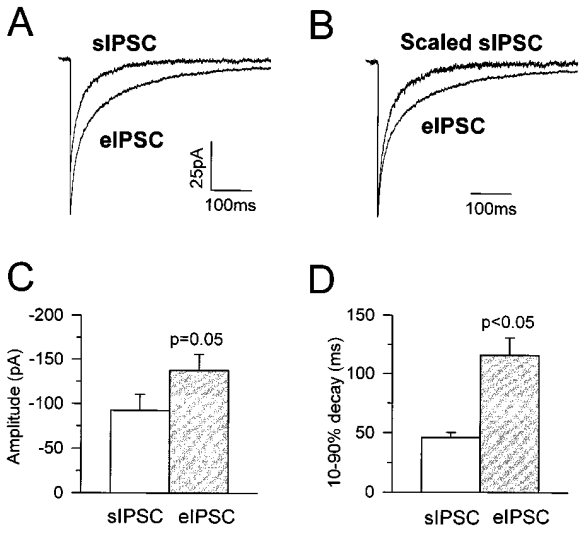

Figure 2. The eIPSC Decays More Slowly than the sIPSC

(A and B) The average of 50 sIPSCs and 65 eIPSCs from the same cell are overlaid in (A) and the sIPSC is scaled to the peak amplitude of the eIPSC in (B) to emphasize the difference in decay rate. The stimulation artifact was blanked on the evoked synaptic current traces.

(C and D) The mean peak amplitude (C) and 10%–90% decay time (D) of the sIPSC and eIPSC in 20 granule cells. Error bars represent SEM.

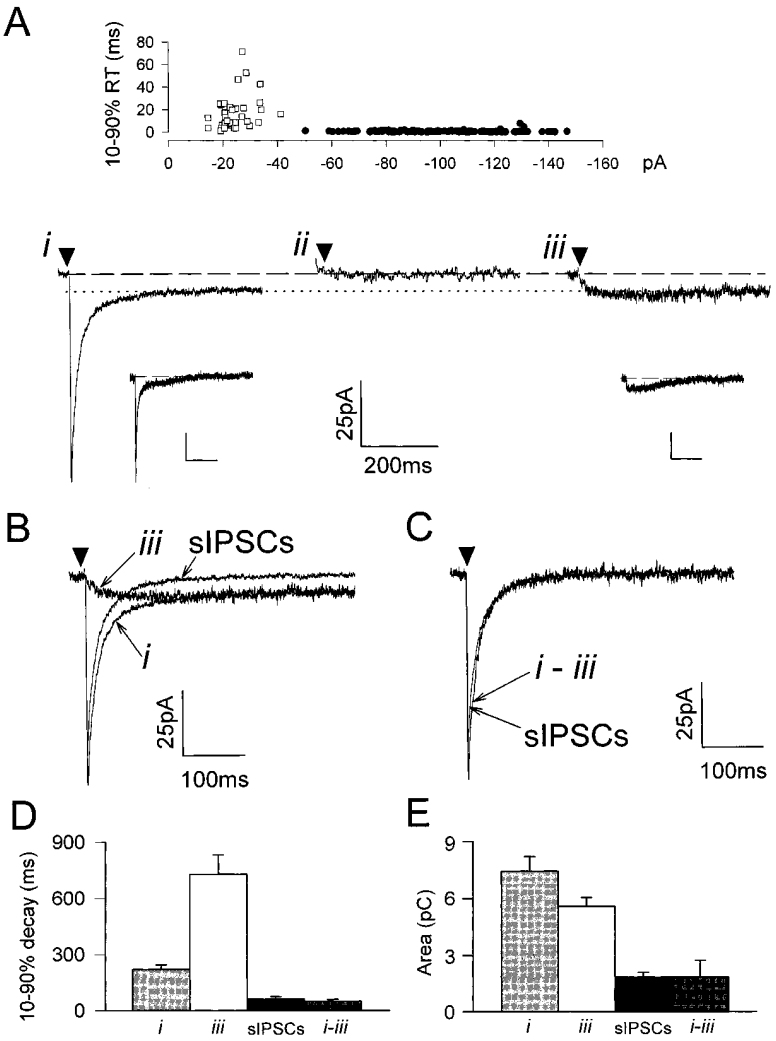

Figure 3. The eIPSC Is Composed of Two Kinetically Distinct Current Components

(A) Electrical stimulation can evoke different current responses in the same cell. At the top, the plot of peak amplitude versus the 10%–90% rise time shows two distinct populations of eIPSC (squares and circles) in the same cell. In addition to failures ([ii], 6 out of 200 responses, shown as an average of the 6 failure responses here), stimulation evoked fast rising currents (circles; 137 of 200 responses, shown as an average of the 137 in [i]) and slow rising currents (squares; 57 of 200 responses, shown as the average of the 57 in [iii]). Insets show the same response at a slower time scale to show that they do eventually decay back to baseline. Calibration bars, 20 pA and 500 ms.

(B) The two types of response (i and iii) are shown superimposed on the averaged sIPSC in the same cell.

(C) The waveform, generated by mathematical subtraction of the isolated slow rising eIPSC (iii) from the isolated fast rising eIPSC (i), is superimposed on the averaged sIPSC.

(D and E) Bar charts display the mean (± SEM) 10%–90% decay time (D) and area (E) of the isolated fast rising eIPSC (i), the isolated slow rising eIPSC (iii), the average of the sIPSC, and the waveform resulting from the mathematical subtraction (as in [C]) of the isolated slow rising eIPSC from the isolated fast rising eIPSC (i–iii) in the same cell ($n = 4$ cells).

Arrowheads in (A) through (C) indicate the time of stimulation. The stimulation artifact was blanked on the evoked synaptic current traces.

well ($p < 0.05$, Spearman's rank correlation test) with the difference in decay rates for the eIPSC and sIPSC measured in the same cell (Figures 4C and 4D). Using the number of discrete steps in the stimulus-intensity response curves for the fast component of the eIPSC (Figure 4B) as an indicator of the number of direct terminals, and the ratio of remote terminals to direct terminals to estimate the number of remote terminals, we calculate that at maximal stimulus strengths a total of 7.2 ± 1.4 (in $n = 12$ granule cells) direct and remote terminals were activated. This represents the lower limit to the total number of terminals influencing a single granule cell. These calculations will be related to the known anatomy of Golgi to granule cell synapses in the Discussion.

Differential Modulation of Fast and Slow IPSCs by Subunit-Specific Compounds

In adult rats, cerebellar granule cells express mRNA for nine different $GABA_A$ receptor subunits (Laurie et al., 1992; Persohn et al., 1992), but the most common receptors expressed are thought to be those containing α_1 and α_6 subunits (Quirk et al., 1994). The α_1 and α_6 subunits of the $GABA_A$ receptor confer different pharmacological sensitivities to benzodiazepines and furosemide. Diazepam has been shown to potentiate selectively α_1-containing receptors (relative to α_6-containing receptors; Saxena and MacDonald, 1996), whereas α_6-containing receptors are selectively inhibited by furosemide (Korpi et al., 1995). We used these compounds to examine the contribution of different receptor subtypes to the fast and slow IPSCs.

Diazepam (500 nM) did not affect the peak amplitude of either the sIPSC or eIPSC ($Wp > 0.05$, $n = 7$) but significantly increased the 10%–90% decay time of both (1.43- ± 0.14-fold, $n = 6$, $Wp < 0.05$, and 1.44- ± 0.18-fold, $n = 7$, $Wp < 0.05$, respectively; Figure 5A). In both cases, the prolongation reflected changes to early components of the current decay (Figure 5A). This prolongation of decay without an effect on the peak of the IPSC is consistent with an increase of the affinity of the receptor for GABA and the receptors being saturated at the peak (Otis and Mody, 1992).

Furosemide (100 μM) did not affect the peak amplitude of either the sIPSC or the eIPSC ($Wp > 0.05$, $n = 7$; Figure 5B). While furosemide did not affect the rate of decay of sIPSCs, it did significantly reduce the 10%–90% decay time of the eIPSC (by 51% ± 6.5%, $n = 7$,

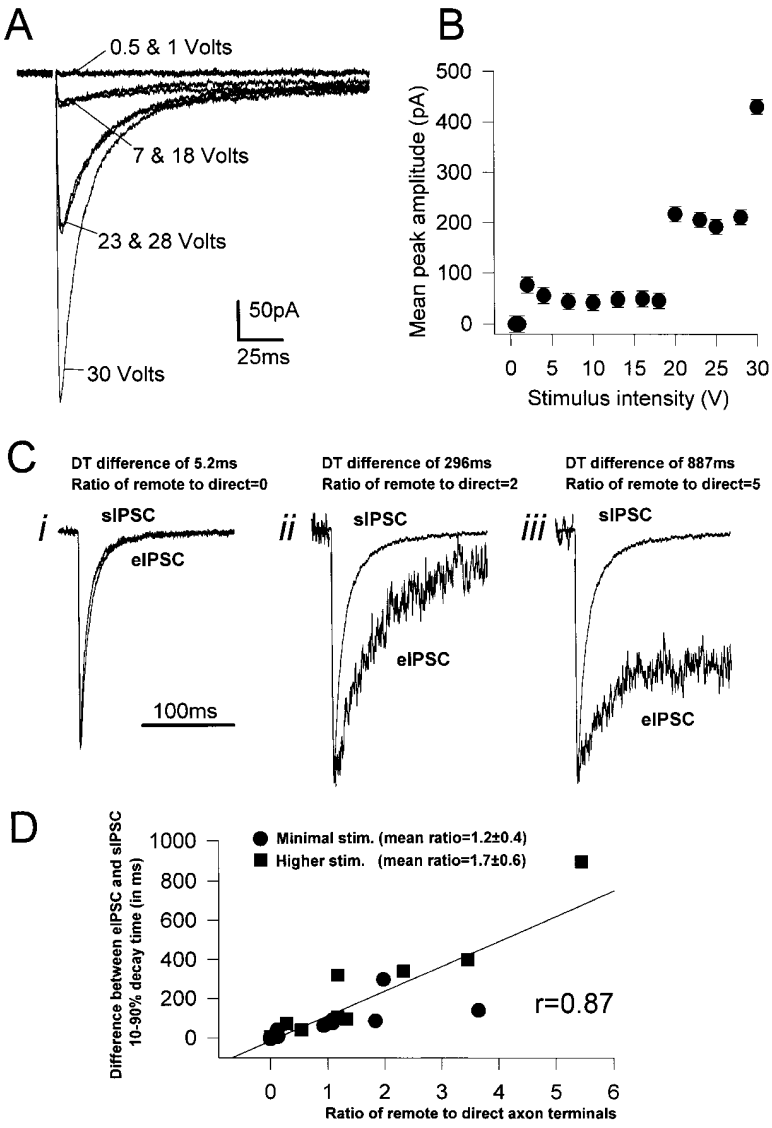

Figure 4. Estimation of the Number of Axon Terminals Underlying the Fast and Slow eIPSCs

(A) Averaged eIPSC (50 responses) at varying stimulus intensities.

(B) Mean peak eIPSC amplitude versus stimulus intensity (same cell as in [A]).

(C) Some examples of averaged sIPSC and eIPSC in two different cells with different calculated ratios of remote to direct terminals (see Experimental Procedures). The sIPSC and eIPSC have been scaled to the same peak amplitude to demonstrate the difference in decay rates. (i) shows an sIPSC and an IPSC evoked at minimal stimulus strength. (ii) and (iii) come from a different cell, and show the sIPSC overlaid with an IPSC evoked at two different stimulus strengths ([ii] being at minimal stimulus strength and [iii] being stronger).

(D) Plot of the difference in the 10%–90% decay time between the eIPSC and the sIPSC versus the calculated ratio of axon terminals underlying the slow and fast eIPSCs. The plot is derived from 10 different cells at both minimal stimulus strength and at the highest stimulus strength that still allowed the calculation to be performed (see Experimental Procedures).

Wp $<$ 0.05; Figure 5B). This decrease in decay time reflected changes to later components of the current decay (Figure 5B). It appears, therefore, that the slow component of the IPSC is generated by α_6-containing $GABA_A$ receptors. Indeed, in three cells where greater than 90% of the responses were slow IPSCs in isolation, they were inhibited by furosemide (peak reduced by 48.8% $\pm$ 7.1%, $p < 0.05$; Figure 5B, inset).

Taken together, these results suggest that the fast rising and decaying component of IPSCs, whether evoked or spontaneous, is mediated largely by receptors with α_1 subunit pharmacology, whereas the additional slow evoked component (Figure 3Aiii and inset, Figure 5B) is mediated by receptors with α_6 subunit pharmacology.

The Neuronal GABA Transporter Antagonist SKF 89976-A Prolongs the Decay of eIPSCs but Not sIPSCs

Next, we examined the role of GABA reuptake in shaping the various components of IPSCs described above. To do this, we used SKF 89976-A, a selective antagonist for the GABA transporter GAT-1 that is not transported by GAT-1 and thus does not promote release of GABA by heteroexchange (Larsson et al., 1988; Solis and Nicoll, 1992). In the cerebellum, GAT-1 is concentrated in the Golgi axon terminals (Itouji et al., 1996). Consequently, SKF 89976-A will specifically block GABA reuptake into the terminals that release it. Application of SKF 89976-A (100 μM) produced a small, tonic inward current (5 $\pm$ 1 pA, n = 8; data not shown, but see Hamann and Rossi, 1997, and Wall and Usowicz, 1997) and an increase of current noise but did not affect the amplitude or kinetics of sIPSCs (n = 10, $p > 0.05$; Figure 6A). SKF 89976-A did, however, affect the eIPSCs. The eIPSC amplitude was significantly decreased (by 31% $\pm$ 3.2%, n = 11, $p < 0.05$; Figure 6B) and its decay was significantly prolonged by SKF 89976-A (1.41- $\pm$ 0.22-fold, n = 11, $p < 0.05$; Figure 6B). The increase in decay was due entirely to a prolongation of the time constant of the slowest component of a double or triple exponential fit

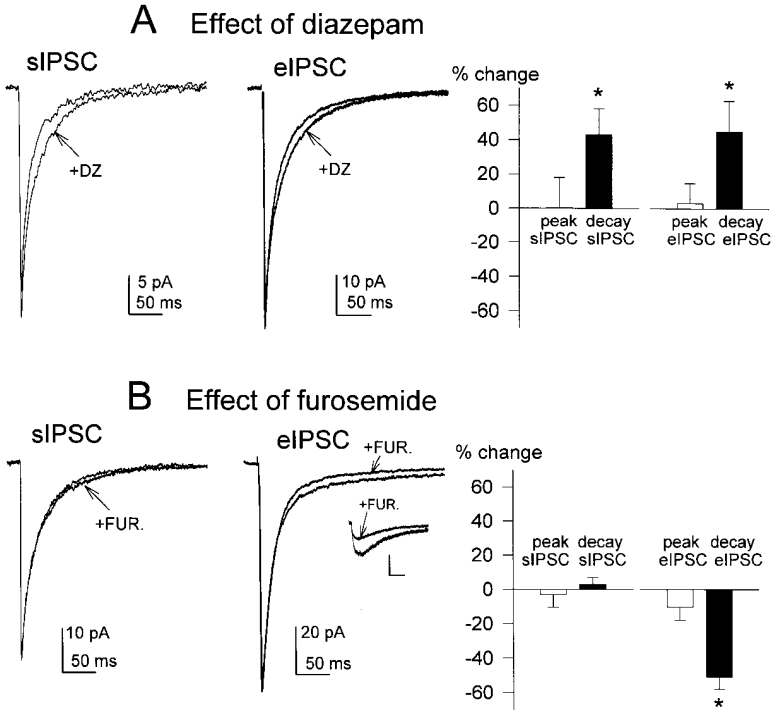

Figure 5. Diazepam and Furosemide Differentially Modulate the Fast and Slow Components of IPSCs

(A) Representative data traces showing the effect of 500 nM diazepam (DZ) on the sIPSC (left) and the eIPSC (middle) in the same cell. The mean percent change in amplitude and 10%–90% decay time produced by diazepam is shown at right (n = 5 for eIPSC, n = 6 for sIPSC). The prolongation of the sIPSC was reflected by a 2.24 ± 0.52 (Wp < 0.05) and 1.54 ± 0.21 (Wp < 0.05) -fold increase in τ_1 and τ_2, respectively in a triple exponential fit. None of the other parameters of the fit were significantly affected. The prolongation of the eIPSC was reflected by a 1.18- ± 0.07-fold increase (Wp < 0.05) in the relative amplitude of τ_1. None of the other parameters of the fit were significantly affected.

(B) Representative data traces showing the effect of 100 μM furosemide (FUR) on the averaged sIPSC (left) and eIPSC (center) in the same cell. The inset shows the effect of furosemide in a different cell that had predominantly isolated slow rising eIPSCs (scale bar, 10 pA and 100 ms). The mean percent change in amplitude and 10%–90% decay time produced by furosemide is shown at right (n = 7 for eIPSC, n = 10 for sIPSC). The asterisk (*) indicates significance (Wp < 0.05) as assessed by a Wilcoxon matched pairs test. The decreased decay time of the eIPSC was reflected by a significant decrease (42.2% ± 12.9%; Wp < 0.05) of the slowest τ value, τ_3. None of the other parameters of the fit were significantly affected.

(τ_3 was increased 2.29- ± 0.31-fold, n = 10, p < 0.05), and the magnitude of the prolongation was proportional to the initial decay rate (r = 0.89, p < 0.05, Spearman's rank correlation test; Figure 6C). None of the other parameters of the two- or three-exponential fit were significantly affected. These results demonstrate that neuronal GABA uptake is a rate-limiting factor in the removal of GABA during the slow component of the eIPSCs.

Spontaneous GABAergic Spillover

If the slow rising eIPSCs are due to release of GABA from remote terminals activated by electrical stimulation and remote terminals have the same release properties as direct terminals, then slow rising IPSCs might be expected to occur spontaneously. Slow rising sIPSCs were observed in some cells (Figure 7A) but were generally difficult to discriminate amid the tonic $GABA_A$ receptor-mediated noise seen in most cells (Figure 7B; see also Puia et al., 1994; Kaneda et al., 1995; Brickley et al., 1996; Wall and Usowicz, 1997). In four cells where slow rising spontaneous IPSCs could be clearly resolved (Figure 7A), they had a mean 10%–90% rise time of 12.3 ± 2.6 ms, a peak amplitude of 10.5 ± 1.9 pA, and a 10%–90% decay time of 279 ± 27.6 ms. The slow rising sIPSCs occurred at a similar frequency to the fast rising sIPSCs in the same cell (frequency = 0.20 ± 0.06 Hz and 0.49 ± 0.27 Hz, respectively, p > 0.05).

GABAergic Spillover at Physiological Temperatures and in Adult Tissue

To determine if the principles uncovered here apply more generally to the function of the glomerulus in vivo, we also recorded from granule cells at physiological temperatures (35°C–37°C) and from adult cerebellum (35 days old). At 35°C–37°C, electrical stimulation reliably (in 10 of 11 cells tested) evoked slow rising (10%–90% rise time = 27.0 ± 8.2 ms), small amplitude (20.6 ± 3.0 pA) IPSCs that were blocked by 10 μM bicuculline (data not shown). Further, the decay of the composite eIPSC was prolonged by application of 100 μM SKF 89976-A (10%–90% decay time increased by 50.0% ± 20.9%, Wp < 0.05, n = 6; data not shown) and shortened by application of 100 μM furosemide (10%–90% decay time decreased by 55.7% ± 12.2%, Wp < 0.05, n = 5; data not shown). Granule cells in adult cerebellar slices also exhibited slow rising (10%–90% rise time = 16.4 ± 4.5 ms, n= 6), small amplitude (18.2 ± 2.8, n = 6) eIPSCs which were blocked by either 10 μM bicuculline (six of six cells) or 1 μM TTX (three of three cells). These results strengthen the case that transmission mediated by GABAergic spillover will occur in adults in vivo.

Discussion

Evoked IPSCs Have Two Components Mediated by Different $GABA_A$ Receptor Subtypes

To date, analysis of inhibitory transmission from Golgi cells to granule cells has focused solely on spontaneously occurring IPSCs (Puia et al., 1994; Kaneda et al., 1995; Brickley et al., 1996; Tia et al., 1996a; Wall and Usowicz, 1997). We show here that evoked IPSCs (eIPSCs) decay much more slowly than spontaneous IPSCs (sIPSCs). This is due to eIPSCs being the sum of slow rising and decaying, small amplitude responses with rapidly rising and decaying, large amplitude events that occur spontaneously (Figure 3). As both responses are completely

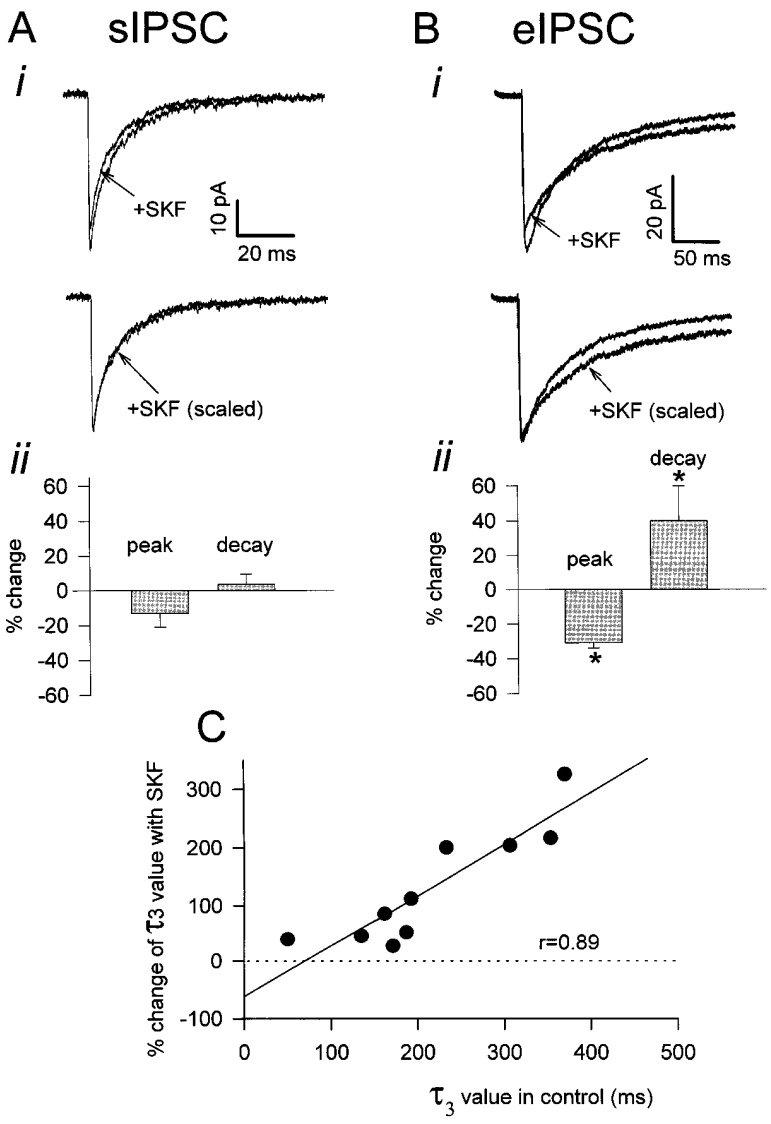

Figure 6. The Neuronal GABA Transporter (GAT-1) Blocker, SKF 89976-A, Prolongs the Decay of the eIPSC but Not of the sIPSC

(A) SKF 89976-A does not affect the sIPSC. Specimen traces showing the lack of effect of 100 μM SKF 89976-A (SKF) on the averaged sIPSC ([Ai], Top). Traces scaled to the same peak amplitude to compare decay rates ([Ai], Bottom). Mean change in peak amplitude and 10%–90% decay time produced by SKF 89976-A (n = 10) (Aii).

(B) SKF 89976-A (100 μM) affects the eIPSC. Specimen traces showing the effect of 100 μM SKF 89976-A (SKF) on the peak amplitude of eIPSC ([Bi], Top). Traces scaled to the same peak amplitude to show the prolongation of the decay ([Bi], Bottom). Mean change in the amplitude and 10%–90% decay time produced by SKF 89976-A (n = 11) (Bii). The asterisk (*) indicates significance ($p < 0.05$) as assessed by a Student's t test.

(C) Plot of the percent change in τ_3 (the slowest time constant of the exponential fit) produced by 100 μM SKF 89976-A versus the initial value of τ_3.

abolished by either bicuculline or TTX, they both represent action potential-dependent release of GABA onto granule cells. Experiments with subunit-specific modulators demonstrate that the slow eIPSCs are generated largely by α_6 subunit-containing $GABA_A$ receptors, whereas the fast eIPSCs are generated by α_1-containing receptors (Figure 5; Korpi et al., 1995; Saxena and MacDonald, 1996). While granule cell sIPSCs reported here (see also Puia et al., 1994; Kaneda et al., 1995; Brickley et al., 1996; Wall and Usowicz, 1997) are similar in pharmacological and kinetic properties to GABAergic IPSCs seen in other cell types throughout the brain (Edwards et al., 1990; Otis and Mody, 1992; Vincent et al., 1992; Pearce, 1993; Llano and Gerschenfeld, 1993; Salin and Prince, 1996), the slow rising small amplitude eIPSCs are novel.

Mechanisms of the Slow IPSC Component

There are several plausible mechanisms that could underlie these slow IPSCs: (1) distortion of fast synaptic currents by cable properties of the cell, (2) novel $GABA_A$ receptor properties unique to cerebellar granule cells, (3) slow release of low concentrations of GABA through a narrow preexocytotic fusion pore (as has been suggested to occur in nonneuronal secretory cells; Chow et al., 1992; Zhou et al., 1996), or (4) GABA spillover from neighboring but not directly connected axon terminals. We favor the GABA spillover hypothesis for the reasons presented below.

Cable Properties

Because of their small size and restricted dendritic field (Figure 1B), granule cells are extremely electrically compact. Modeling suggests that granule cell cable properties produce very little distortion of synaptic currents (Silver et al., 1992, 1996; Gabbiani et al., 1994). Even if some distortion were to occur, the fact that all of the known synapses onto granule cells occur at the distal tips of their dendrites, which are of similar length and caliber, means that all synaptic currents should be similarly distorted. Thus, it is unlikely that distortion of currents by cable propagation can account for the observed difference in kinetics of the two components of the IPSC.

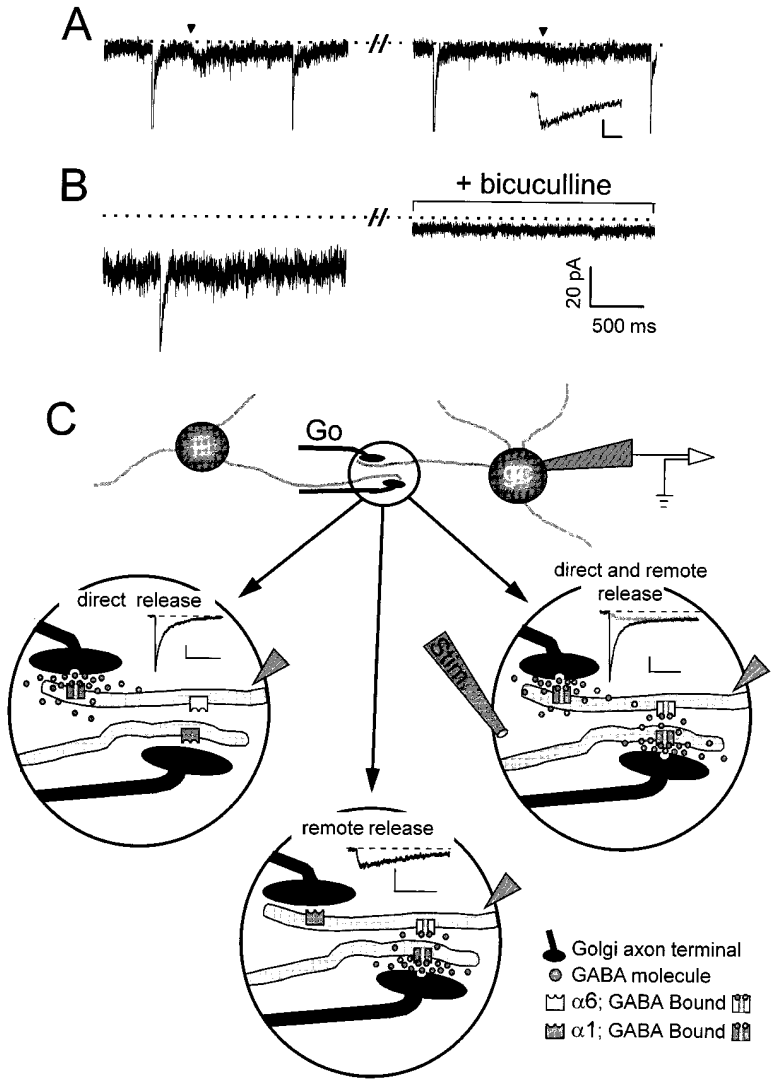

Figure 7. Schematic Representation of Spillover at the Golgi Cell to Granule Cell Synapse

(A) Continuous recording illustrates spontaneous slow rising, small amplitude IPSCs (arrowheads) as well as more typical sIPSCs in the same cell. The average of 25 of the former events is shown in the inset (scale bar, 4 pA and 50 ms).

(B) Tonic $GABA_A$ receptor-mediated conductance is blocked by 10 μM bicuculline.

(C) Within the glomerulus (enlarged in the three panels), Golgi cell axon terminals (Go) form synapses with granule cells (gc). Fast rising IPSCs are produced by release of GABA from directly connected Golgi axon terminals. This can occur spontaneously as at left or when evoked by electrical stimulation as shown at right (black inset). Electrical stimulation also evokes GABA release from remote terminals which spills out and generates the slow decaying tail of the eIPSCs (compare decay rates of the sIPSC and the eIPSC shown at left and right, respectively; scale bar, 100 ms and 20 pA). In the absence of release from directly connected terminals, release of GABA from remote terminals generates slow rising small amplitude IPSCs. This occurs in response to electrical stimulation when the direct terminal fails to release (gray inset, right) and can also occur spontaneously (inset, bottom). Fast rising IPSCs are generated by activation of α_1-containing $GABA_A$ receptors in the postsynaptic membrane of the granule cell. Slow rising IPSCs are generated by extrasynaptic high affinity α_6-containing $GABA_A$ receptors which sense low concentrations of GABA spilling out of remote synapses. The arrowhead points to the dendrite of the granule cell being recorded.

Receptor Properties

Our data show clearly that the fast and slow IPSCs are largely generated by distinct $GABA_A$ receptor subtypes (Figure 5). Could inherently different kinetic properties of these distinct receptor subtypes account for the different IPSC waveforms? There have been numerous studies of recombinantly expressed $GABA_A$ receptors with different subunit combinations. These studies show that different subunit combinations impart distinct pharmacological and kinetic properties to the receptor (Korpi et al., 1995; Saxena and MacDonald, 1996; Tia et al., 1996b; Wisden et al., 1996; Zhu et al., 1996). However, none of these subunit combinations result in $GABA_A$ receptors with slow activation kinetics. In fact, all of the combinations most likely to occur in cerebellar granule cells (e.g., $\alpha_1\beta_x\gamma_2$, $\alpha_6\beta_x\gamma_2$, and $\alpha_6\beta_x\delta$ in adult) display rapid activation kinetics despite having different affinities and pharmacological sensitivities (Ducic et al., 1995; Korpi et al., 1995; Saxena and MacDonald, 1996; Tia et al., 1996b). Further, at concentrations of GABA thought to be released into the synaptic cleft, the activation kinetics of endogenous $GABA_A$ receptors in granule cell patches are rapid (Maconochie et al., 1994).

A Low and Slow [GABA] Rise

An alternative possibility is that in a subset of synapses, lower concentrations of GABA are released into the cleft. At lower concentrations of GABA, both hippocampal and cerebellar $GABA_A$ receptors display significantly slower activation kinetics (Maconochie et al., 1994; Jones and Westbrook, 1995). However, if we compare the average activation rate of our slow IPSCs with the dose-response curve for granule cell $GABA_A$ receptor activation rates of Maconochie et al. (1994), we find that our slow eIPSC activation rate would be generated by a concentration of 10 μM, a dose of GABA that produces a nearly maximal response amplitude (but not a maximal onset rate). Therefore, to account for both the small amplitude of the slow component relative to the fast one, and the slow onset of the slow eIPSCs, we would have to propose a small number of receptors as well as a low peak GABA concentration. Furthermore, low concentrations of GABA are not expected to generate longer decay times (Maconochie et al., 1994; Jones and Westbrook, 1995). Therefore, the most likely explanation of the slow rise and decay time of the slow eIPSCs is that the GABA concentration that produces them rises

and falls with a prolonged time course. This is further supported by the prolongation of decay time produced by blocking GABA uptake (Figure 6). Although it has been suggested that transmitter can be released slowly from a preexocytotic fusion pore in the absence of full vesicular fusion (Chow et al., 1992; Zhou et al., 1996), recent calculations based on the conductance of chromaffin cell fusion pores suggest that most of the contents of the much smaller synaptic vesicle would be released in less than 1 ms (Albillos et al., 1997).

Spillover

Finally, two analytical diffusion models (Crank, 1975; Barbour and Häusser, 1997; see Experimental Procedures) predict that for distances of the order of the glomerulus radius ($\sim$2.5 μm) GABA will spill over at concentrations sufficient to activate α_6-containing receptors. Estimates of vesicular transmitter content range from 1000 molecules for GABA, through 2000 molecules for glutamate, to 7500 molecules for acetylcholine (Edwards, 1995). If we assume 1000 GABA molecules are released into an infinite disc of 20 nm thickness, then 6 ms (the half rise time of the slow eIPSCs) after release the concentration of GABA will still be 1 μM (the EC_{50} of α_6-containing receptors; Saxena and MacDonald, 1996) at a radius of 2.6 μm (from equation 2 of Experimental Procedures). However, the model of the extracellular space as an infinite disk becomes less accurate as more branch points are added to the diffusional path. Since any extracellular path across the glomerulus will have multiple branch points, we also used the analytical solution for diffusion in a three-dimensional porous medium (equation 3; Crank, 1975; Barbour and Häusser, 1997). This predicts that by 6 ms after release, at a distance of 2.6 μm, the GABA concentration will be 679 nM. This concentration of GABA would produce 16%–81% of the maximal possible response for the various α_6-containing $GABA_A$ receptors while producing only 0%–2% of the maximal response for α_1-containing receptors (as determined from the dose-response curves for recombinantly expressed $GABA_A$ receptors; Saxena and MacDonald, 1996). Although the distance GABA diffuses will be reduced by binding to GABA transporters in the presynaptic terminal (Itouji et al., 1996; Barbour and Häusser, 1997), there are numerous granule cell dendrites even within 1 μm of a given Golgi-granule cell synapse (Hámori and Szentágothai, 1966; Jakab and Hámori, 1988; Jakab, 1989). Furthermore, if we take the higher estimate of 7500 transmitter molecules per vesicle, by 6 ms after release even the cleft concentration right at the release site will have dropped below 13 μM (from equation 2), the approximate EC_{50} for several different α_1-containing receptors (Saxena and MacDonald, 1996). These numbers fit well with our suggestion that the slowly rising, long lasting eIPSCs are generated by GABA spilling over a distance comparable to the glomerular radius to activate receptors with α_6 subunit pharmacology. The fact that blocking neuronal GABA uptake prolongs the decay of the slow component of the eIPSC is also consistent with it being generated by transmitter spillover (Isaacson et al., 1993; Asztely et al., 1997). Consistent with the glomerular geometries' capacity to trap GABA released by electrical stimulation, recent observations of a tonic current generated by spontaneous, TTX-sensitive GABA release onto granule cells were interpreted in terms of GABA accumulation in the glomerulus (Wall and Usowicz, 1996, 1997; Brickley et al., 1996).

The Number of Direct and Remote Inputs to Each Granule Cell

The granule cells from which we recorded had one to eight dendrites (mean = 3.0 $\pm$ 0.22, n = 42; Figure 1B). In the adult rat cerebellum, each granule cell dendrite receives 2.6 $\pm$ 0.55 synaptic contacts from Golgi axon terminals (Jakab and Hámori, 1988). These numbers imply that each granule cell is contacted, at most, by a mean of 7.8 distinct Golgi axons. This number would be less if any of the 2.6 synaptic contacts are from the same Golgi axon and may be further reduced if the number of Golgi cell–granule cell synapses is somewhat less in the 12-day-old rat than we have used in this study (Hámori and Somogyi, 1983). Based on the number of steps in our stimulus intensity response curves and the estimated ratio of remote to direct axon terminals, we found that at maximal stimulus intensities 7.2 $\pm$ 1.4 distinct (direct and remote) inputs were stimulated (Figure 4). This should be viewed as an underestimate of the total number of direct and remote inputs to a single granule cell, for the following reasons. First, we were unable to calculate the ratio of remote to direct inputs at maximal stimulation intensities due to the lack of fast IPSC failures. If we extrapolate to maximal stimulation intensities by assuming that the ratio of remote to direct inputs stays the same (as it did at minimal and higher stimulus intensities; Figure 4D), then with a remote to direct ratio of 1.7 the total number of direct and remote terminals is calculated to be 8.9 $\pm$ 2.0. Further, because the granule cell dendrites are symmetrically distributed around the cell soma, it is likely that at maximal stimulus intensities (beyond which cell disruption occurs) we do not stimulate all of the available inputs. Thus, the total number of axon terminals that give rise to fast and slow IPSCs probably exceeds the number of axon terminals directly connected to a single granule cell. This discrepancy can best be accounted for by the spillover hypothesis (Figure 7).

Spontaneous GABAergic Spillover

If each granule cell has roughly equal numbers of remote and direct terminals to which it can respond (Figure 4D), and if remote terminals have similar release properties to those of directly connected terminals, then an obvious prediction of our model is that slow rising IPSCs generated by GABA spillover from remote terminals should occur spontaneously. Slow rising sIPSCs are indeed observed (Figure 7A) but are relatively infrequent. There are several reasons why this may be so. First, spillover generated IPSCs, whether evoked (Figure 3Aiii) or spontaneous (Figure 7A), have a small peak amplitude and slow rise time, making it difficult to discriminate confidently such events from the tonic conductances of the cell (Figure 7B; see also Kaneda et al., 1995; Brickley et al., 1996; Wall and Usowicz, 1997) when they are not time locked with an obvious marker like a stimulation

artifact. Additionally, the tonic $GABA_A$ receptor-mediated conductance of granule cells (Figure 7B), which has been interpreted as GABA spillover because of its sensitivity to TTX (Brickley et al., 1996; Wall and Usowicz, 1997), may actually be multiple, asynchronously overlapping, small amplitude, long-lasting, spillover-mediated IPSCs.

Importance of the α_6 Subunit

We suggest that when GABA is released from Golgi cells into the Golgi cell-granule cell synaptic cleft, it activates α_1-containing $GABA_A$ receptors in the postsynaptic membrane of the granule cell and generates a typical IPSC (Figure 7C, left; Edwards et al., 1990; Vincent et al., 1992; Otis and Mody, 1992; Pearce, 1993; Llano and Gerschenfeld, 1993; Salin and Prince, 1996). However, unlike at other inhibitory synapses, as GABA diffuses out of the synaptic cleft, it encounters other dendritic processes that contain high-affinity α_6-containing $GABA_A$ receptors, thus generating slow IPSCs in neighboring cells (Figure 7C, right and bottom).

One inconsistency with our data is that Nusser et al. (1996) showed that the α_6 subunit is concentrated in the synaptic cleft and yet furosemide was without effect on the fast rising IPSCs (Figure 5B; see also Puia et al., 1994). This apparent discrepancy may arise from the differences in the age of the animals used. Nusser et al. (1996) studied adult rats, whereas we mainly studied 12-day-old rats, an age at which the α_6 subunit is just being expressed (Zheng et al., 1993; Varecka et al., 1994). In fact, at older ages, furosemide does produce a small block of sIPSCs (Tia et al., 1996a). Thus, α_6 may initially be expressed at extrasynaptic sites and become concentrated in the synaptic cleft as development proceeds. Spillovers still occur in the adult (see Results) and thus may result from GABA released at one synapse activating α_6-containing receptors that either remain in an extrasynaptic location or are postsynaptic at another synapse nearby (Nusser et al., 1996). Alternatively, because the δ subunit is expressed only extrasynaptically (Nusser et al., 1998), spillover-generated IPSCs may be mediated by $GABA_A$ receptors comprised of $\alpha_6\beta_3\delta$ subunits. Indeed, $GABA_A$ receptors containing these subunits make up 23% of all the $GABA_A$ receptors found in granule cells (Quirk et al., 1994) and have the highest affinity for GABA (EC_{50} = 0.27 μM; Saxena et al., 1996).

Isaacson et al. (1993) showed that during high frequency stimulation of hippocampal CA1 afferents GABA can spill out of the synapse and activate $GABA_B$ receptors on neighboring presynaptic glutamatergic terminals. However, activation of heterosynaptic $GABA_A$ receptors was not observed. Based on their model of hippocampal CA1 $GABA_A$ receptors, Jones and Westbrook (1995) suggested that entry into a monoliganded desensitized state could attenuate responses to slowly rising, low concentrations of GABA and hence mask responses to spillover of GABA. This mechanism may be circumvented in the granule cell because the α_6-containing receptors have a higher affinity for GABA (and so are more likely to pass into the di-liganded state which leads to channel opening) and do not readily desensitize (Tia et al., 1996b).

Importance of the Neuronal GABA Transporter GAT-1

A high affinity neuronal GABA transporter (GAT-1) is known to be present in the cerebellar Golgi cell terminals (Itouji et al., 1996). We found that the inhibition of neuronal GABA uptake by SKF 89976-A did not affect spontaneous IPSCs (Figure 6A). A similar lack of effect on miniature or spontaneous IPSCs was also observed in hippocampal CA1 pyramidal cells (Thompson and Gähwiler, 1992; Isaacson et al., 1993). In contrast, SKF 89976-A prolonged the decay of the late phase of evoked IPSCs in granule cells (Figures 6B and 6C). In the hippocampus, strong, repetitive stimulation of the GABAergic afferents causes a spillover of GABA to neighboring presynaptic excitatory terminals that activates high affinity $GABA_B$ receptors and thereby inhibits excitatory transmission (Isaacson et al., 1993). This effect is also enhanced by SKF 89976-A.

These findings suggest that, generally, when GABA is released by a single terminal its removal by diffusion is rapid and the decay of the IPSC is determined by channel kinetics. However, under conditions that promote spillover, such as those reported here or during repetitive stimulations in the hippocampus, GABA reuptake is an important factor in limiting the magnitude of such spillover.

In the glomerulus, blocking neuronal GABA uptake with SKF 89976-A results in an accumulation of synaptically released GABA at a concentration sufficient to activate $GABA_A$ receptors and generate a tonic inward current (see Results; Wall and Usowicz, 1996, 1997). Thus, the decrease in amplitude of the eIPSC in the presence of SKF 89976-A is likely due to either occupation or desensitization of $GABA_A$ receptors, or both, or to a decrease in release of GABA as a result of activation of presynaptic $GABA_B$ receptors. If any combination of these actions occurs, then a similar decrease in amplitude of the sIPSC would be expected. While SKF 89976-A did decrease the mean amplitude of the sIPSC, the decrement failed to reach significance (Figure 6A). This is probably because the SKF 89976-A–induced noise hinders detection of small sIPSCs that are not time locked with respect to some known marker like a stimulation artifact for eIPSCs. Consequently, in the presence of SKF 89976-A, the amplitude of the average sIPSC is probably an overestimate of the actual value as the smallest events are excluded from the average.

Functional Significance of Intraglomerular GABA Spillover

From an anatomical perspective, the glomerulus seems designed to promote heterosynaptic spillover of GABA. We have shown that such spillover occurs. Although the amplitude of the slow rising IPSCs is small (Figure 3A), the long duration of these events results in a total charge transfer that is three times greater than that of the IPSCs generated by directly connected terminals (Figure 3E). Further, at a holding potential of −60 mV, the mean peak amplitude of isolated slow rising IPSCs was 17.3 ± 2.7 pA. With the calculated reversal potential of 0.5 mV, this corresponds to a peak conductance of 282 pS. Because of the extremely compact size of granule cells (Figure

1B), a relatively small change in input conductance can significantly alter the way in which they respond to excitatory inputs (Gabbiani et al., 1994; Brickley et al., 1996). In fact, Brickley et al. (1996) showed that blocking a tonic $GABA_A$ receptor-mediated conductance of about 150 pS was enough to alter significantly the action potential response to current injection. Therefore, even isolated GABA spillover-generated currents could alter the input-output relationship of granule cells.

GABAergic synaptic inputs to the interneurons of the cerebellar molecular layer can influence synaptic integration by changing the membrane time constant (Häusser and Clark, 1997), and models of cerebellar granule cells suggest a similar role for a tonic GABAergic input (Gabbiani et al., 1994). With physiological intracellular solution (low chloride, potassium based), the granule cell input resistance and membrane capacitance are 2.3 ± 1.1 GΩ and 3.1 ± 1.5 pF, respectively, giving a membrane time constant of 6.7 ms (D'Angelo et al., 1995). The peak conductance generated by GABA spillover would change this value to 4.3 ms. This change in time constant covers the lower part of the range of firing frequencies of mossy fibers (20–120 Hz; Lisberger and Fuchs, 1978) and thus will likely be an important factor in setting the time window for input integration.

Theoretical models suggest that cerebellar information processing is optimized if there is sparse coding of information by the array of granule cells (Marr, 1969; Tyrrell and Wilshaw, 1992). This implies a relatively small fraction of granule cells being active at any one time, and hence a mechanism by which granule cell excitability is dampened down as more granule cells fire action potentials. It is thought that the granule cell-Golgi cell-granule cell inhibitory feedback loop provides such a mechanism (Marr, 1969; Tyrrell and Wilshaw, 1992). Spillover may make a crucial contribution to this regulation of granule cell excitability, both by increasing the number of Golgi cells (and hence the size of the granule cell pool) feeding back information to inhibit a given granule cell, and also by utilizing the temporal filtering inherent in diffusion across the glomerulus to provide an inhibitory signal that lasts 2.5-fold longer than a conventional fast IPSC.

Experimental Procedures

Preparation of Brain Slices

Patch-clamp recordings from visually identified granule cells in thin (200 μm) parasagittal cerebellar slices obtained from Sprague-Dawley rats were performed as previously described (Edwards et al., 1989; Rossi and Slater, 1993). Slices were obtained from animals of either sex, age 12–15 days postnatal, and maintained at room temperature (~23°C) in an extracellular solution containing (in mM): 126 NaCl, 24 $NaHCO_3$, 1 NaH_2PO_4, 2.5 KCl, 2.5 $CaCl_2$, 10 D-glucose, and 2 $MgCl_2$ bubbled with 95% O_2/5% CO_2 (pH 7.4). In some experiments, 35-day-old rats were used. For recording, slices were placed in a submersion chamber on the stage of an upright microscope and viewed with a Zeiss 40× (0.75 numerical aperture) water immersion objective with Hoffman Contrast Optics. Kynurenic acid (1 mM) was included in the dissection and incubation solution (to block glutamate receptors in an attempt to reduce potential excitotoxic damage) but was omitted from the superfusion solution.

Patch-Clamp Recording and Synaptic Stimulation

Patch recording pipettes were constructed from thick-walled borosilicate glass capillaries (resistance 6–12 MΩ) and filled with an internal solution containing (in mM): 140 CsCl, 4 NaCl, 0.5 $CaCl_2$, 10 HEPES, 0.1 EGTA, 2 MgATP, and 0.5 NaGTP (pH 7.2). Lucifer yellow (0.2%) was added to the internal solution to confirm visual identification of granule cells (Figure 1B). In most experiments, QX-314 (10 mM) was added to the internal solution (with an equiosmolar reduction of CsCl) to block sodium channels and $GABA_B$ receptor-modulated potassium channels. Unless otherwise stated, the holding potential was −60 mV. Membrane currents were acquired at 10–20 kHz, filtered at 5–10 kHz, and analyzed with pClamp (v.6.3) software (Axon Instruments, Foster City, CA) and software written by Stephen Traynelis (Emory University, Atlanta). Unless specified otherwise, 20–100 events were averaged for analysis, and traces were filtered at 1–2 kHz for display.

Borosilicate glass stimulating electrodes (resistance ~1 MΩ) filled with NaCl (1 M) were placed in the granule cell layer, near the granule cell being recorded (<150 μm), in a position that evoked a stable response. Stimuli of 100–400 μs and varying voltage were used at 0.3 Hz to evoke IPSCs that were identified by their subsequent blockade by bicuculline methiodide (10 μM). Glutamate receptor antagonists were not used because they increase the frequency of occurrence of sIPSCs by an unknown mechanism (data not shown). However, all cells that displayed residual synaptic currents in the presence of bicuculline were excluded from analysis. Stimulus intensity-response curves (Figure 4B) were used to establish minimal stimulation parameters (Stevens and Wang, 1994). These curves were generated from the peak of the fast rising eIPSCs (Figure 4A) and should, therefore, represent the activation of a single axon that is directly connected to the recorded cell and an unknown number of remote axon terminals.

All drugs were purchased from Sigma except for QX-314, purchased from Alomone labs, and SKF 89976-A which was a gift from SmithKline Beecham Pharmaceuticals. Furosemide was used at a concentration (100 μM) shown to be selective for the α_6 versus the α_1 subunit of the $GABA_A$ receptor (Korpi et al., 1995) and below that shown to affect Cl^- transport (Misgeld et al., 1986). Drugs were dissolved either directly into Ringer's or in DMSO (final DMSO concentration was 0.1%, which alone did not affect IPSC frequency, amplitude, or kinetics; $P < 0$, $n = 7$ cells).

Calculations

In the rat, all known inhibitory inputs to granule cells are provided by Golgi cells. Therefore, we assume that all eIPSCs are due to GABA release from the same type of terminal, but we suggest that different terminals can generate fast or slow IPSC components depending on whether they are immediately presynaptic to, or at some distance from, the recorded cell (referred to as direct or remote terminals, respectively). We further assume that each Golgi terminal has the same number of release sites (n), with the same probability of release (p), so that the probability of any one fiber failing is $(1 - p)^n$. The probability that there is no fast or no slow IPSC (because all the direct or all the remote terminals fail) will then be $F = [(1 - p)^n]^d$ and $S = [(1 - p)^n]^r$, respectively, where d and r are the number of direct and remote terminals. Thus, the probability that both the slow and fast IPSCs will fail completely is $T = FS = [(1 - p)^n]^{d+r}$. As we know both the proportion of fast IPSC failure (F) and the proportion of total failures (T), we can rearrange the above equations to calculate the ratio of numbers of the two terminal types present: $r/d = (\log T/\log F) - 1$. We then use the number of steps in the stimulus intensity–response curve for the fast IPSC (Figure 4B) as the number of direct terminals, and use the calculated ratio of r/d to estimate the number of remote terminals. At higher stimulus intensities, a fast IPSC was often seen on all trials (because so many terminals are excited that the chance of them all failing becomes negligible), and it is then impossible to do the calculation of terminal-type ratio. Consequently, the number of remote terminals could only be calculated at the highest step on the amplitude response curve that still exhibited fast IPSC failures, and so it is likely to be an underestimate.

When a diffusing substance is released at a point source into an infinite volume, the time it takes to reach half of the peak concentration at a given distance can be described by the equation

$$t_{1/2} = r^2/13.75X \quad (1)$$

as derived from Crank (1975, equation 3.5), where r is the radius of a sphere and X is the diffusion coefficient divided by the tortuosity of the diffusional path (see below for values used). Because the dose-response relationship of the $GABA_A$ receptor is exponential, the use of the half rise time of the synaptic current as an indicator of the time to half peak concentration of GABA will give an overestimate of the actual distance.

At short distances, the extracellular space can be modeled (for diffusion) as a two-dimensional disk of fixed thickness (Barbour and Häusser, 1997). The concentration of GABA at different distances and times after release is then given by

$$C(r,t) = [V/(4\pi DTt)]\exp[-r^2/(4Dt)] \quad (2)$$

where C, the transmitter concentration, is a function of time after vesicular release, t, and distance from the release site, r (Crank, 1975; Barbour and Häusser, 1997). V is the total amount of transmitter released and D is the diffusion coefficient (we used the value 0.76×10^{-9} m^2/s as determined for glutamine; Longsworth, 1953). T is the thickness of the disk in which the molecules are diffusing (we used 20 nm; Barbour and Häusser, 1997).

At greater distances, the extracellular space is better represented as a three-dimensional porous medium for which the concentration is given by

$$C(r,t) = [V/8\alpha\{\pi(D/\lambda^2)t\}^{3/2}]\exp[-r^2/\{4(D/\lambda^2)t\}] \quad (3)$$

(Crank, 1975; Barbour and Häusser, 1997), where α and λ are the volume fraction and tortuosity of the extracellular space, respectively. We use the values $\alpha = 0.21$ and $\lambda = 1.55$ as determined by Nicholson and Phillips (1981) for the cerebellum.

All data are expressed as the mean ± SEM; statistical significance was determined using a Student's t test (p) when the populations seemed normally distributed (i.e., a distribution that was symmetrical about the mean and had variance less than the mean) and the variance of each sample differed by less than a factor of 4. When this was not the case or when the sample size was too small to estimate normality ($n = 5$–10), the nonparametric Wilcoxon matched pairs test (p value represented as Wp) was used. Differences were considered significant when $p \leq 0.05$.

Acknowledgments

We would like to thank D. Attwell, in whose lab this work was done, for his invaluable advice and constructive discussions; D. Becker for the generation of the image of the granule cell; and S. Brickley, M. Catsicas, B. Clark, F. Edwards, M. Farrant, M. Häusser, P. Mobbs, and A. Silver for their critical review of the manuscript. This work was supported by a Wellcome Trust grant to D. Attwell and P. Mobbs.

Received December 5, 1997; revised February 6, 1998.

References

Albillos, A., Dernick, G., Horstmann, H., Almers, W., Alvarez de Toledo, G., and Lindau, M. (1997). The exocytotic event in chromaffin cells revealed by patch amperometry. Nature *389*, 509–512.

Asztely, F., Erdemli, G., and Kullmann, D.M. (1997). Extrasynaptic glutamate spillover in the hippocampus: dependence on temperature and the role of active glutamate uptake. Neuron *18*, 281–293.

Barbour, B., and Häusser, M. (1997). Intersynaptic diffusion of neurotransmitter. Trends Neurosci. *20*, 377–384.

Barbour, B., Keller, B.U., Llano, I., and Marty, A. (1994). Prolonged presence of glutamate during excitatory synaptic transmission to cerebellar Purkinje cells. Neuron *12*, 1331–1343.

Brickley, S.G., Cull-Candy, S.G., and Farrant, M. (1996). Development of a tonic form of synaptic inhibition in rat cerebellar granule cells resulting from persistent activation of $GABA_A$ receptors. J. Physiol. *497*, 753–759.

Chow, R.H., von Rüden, L., and Neher, E. (1992). Delay in vesicle fusion revealed by electrochemical monitoring of single secretory events in adrenal chromaffin cells. Nature *356*, 60–63.

Clements, J.D. (1996). Transmitter timecourse in the synaptic cleft: its role in central synaptic function. Trends Neurosci. *19*, 163–171.

Crank, J. (1975) The Mathematics of Diffusion, 2nd Ed., (Oxford: Oxford University Press).

D'Angelo, E.D., DeFilippi, G., Rossi, P., and Taglietti, V. (1995). Synaptic excitation of individual rat cerebellar granule cells in situ: evidence for the role of NMDA receptors. J. Physiol. *484*, 397–413.

Ducic, I, Carnuncho, H.J., Zhu, W.J., Vicini, S., and Costa, E. (1995). γ-aminobutyric acid gating Cl^- channels in recombinant $GABA_A$ receptors. J. Pharmacol. Exp. Ther. *272*, 438–485.

Edwards, F. (1995). Anatomy and electrophysiology of fast central synapses lead to a structural model for long-term potentiation. Physiol. Rev. *75*, 759–787.

Edwards, F.A., Konnerth, A., Sakmann, B., and Takahashi, T. (1989). A thin slice preparation for patch clamp recording from neurones of the mammalian central nervous system. Pflügers Arch. *414*, 600–612.

Edwards, F.A., Konnerth, A., and Sakmann, B. (1990). Quantal analysis of inhibitory synaptic transmission in the dentate gyrus of rat hippocampal slices: a patch-clamp study. J. Physiol. *430*, 213–249.

Gabbiani, F., Midtgaard, J., and Knöpfel, T. (1994). Synaptic integration in a model of cerebellar granule cells. J. Neurophysiol. *72*, 999–1009.

Hamann, M., and Rossi D.J. (1997). Different roles of neuronal and glial GABA transporters in rat cerebellar slices. J. Physiol. *501*, 13P.

Hámori, J., and Szentágothai, J. (1966). Participation of golgi neuron processes in the cerebellar glomeruli: an electron microscope study. Exp. Brain Res. *2*, 35–48.

Hámori, J. and Somogyi, J. (1983). Differentiation of cerebellar mossy fiber synapses in the rat: a quantitative electron microscope study. J. Comp. Neurol. *220*, 365–367.

Häusser, M. and Clark, B.A. (1997) Tonic synaptic inhibition modulates neuronal output pattern and spatiotemporal synaptic integration. Neuron *19*, 665–678.

Isaacson, J.S., Solís, J.M., and Nicoll, R.A. (1993). Local and diffuse synaptic actions of GABA in the hippocampus. Neuron *10*, 165–175.

Itouji, A., Sakai, N., Tanaka, C., and Saito, N. (1996). Neuronal and glial localization of two GABA transporters (GAT1 and GAT3) in the rat cerebellum. Mol. Brain Res. *37*, 309–316.

Jakab, R.L. (1989). Three-dimensional reconstruction and synaptic architecture of cerebellar glomeruli in the rat. Acta Morphol. Hung. *37*, 11–20.

Jakab, R.L., and Hámori, J. (1988). Quantitative morphology and synaptology of cerebellar glomeruli in the rat. Anat. Embryol. *179*, 81–88.

Jones, M.V., and Westbrook, G.L. (1995). Desensitized states prolong $GABA_A$ channel responses to brief agonist pulses. Neuron *15*, 181–191.

Kaneda, M., Farrant, M., and Cull-Candy, S.G. (1995) Whole-cell and single-channel currents activated by GABA and glycine in granule cells of the rat cerebellum. J. Physiol. *485*, 419–435.

Korpi, E.R., Kuner, T., Seeburg, P.H., and Lüddens, H. (1995). Selective antagonist for the cerebellar granule cell-specific γ-aminobutyric acid type A receptor. Mol. Pharmacol. *47*, 283–289.

Kullmann, D.M., Erdemli, G., and Asztély, F. (1996). LTP of AMPA and NMDA receptor-mediated signals: evidence for presynaptic expression and extrasynaptic glutamate spill-over. Neuron *17*, 461–474.

Larsson, O.M., Falch, E., Krogsgaard-Larsen, P., and Schousboe, A. (1988). Kinetic characterization of inhibition of gamma-aminobutyric acid uptake into cultured neurons and astrocytes by 4,4-diphenyl-3-butenyl derivatives of nipecotic acid and guvacine. J. Neurochem. *50*, 818–823.

Laurie, D.J., Seeburg, P.H., and Wisden, W. (1992). The distribution of 13 $GABA_A$ receptor subunit mRNAs in the rat brain. II. Olfactory bulb and cerebellum. J Neurosci. *12*, 1063–1076.

Lisberger, S.G., and Fuchs, A.F. (1978) Role of primate flocculus during rapid behavioral modification of vestibuloocular reflex. II. Mossy fiber firing patterns during horizontal head rotation and eye movement. J. Neurophysiol. *41*, 764–777.

Llano, I., and Gerschenfeld, H.M. (1993). Inhibitory synaptic currrents in stellate cells of rat cerebellar slices. J. Physiol. *468*, 177–200.

Longsworth, L.G. (1953). Diffusion measurements at 25° of aqueous solutions of amino acids, peptides and sugars. J. Am. Chem. Soc. *75*, 5705–5709.

Maconochie, D.M., Zempel, J.M., and Steinbach, J.H. (1994). How quickly can $GABA_A$ receptors open? Neuron *12*, 61–71.

Malenka, R.C., and Nicoll., R.A. (1997). Silent synapses speak up. Neuron *19*, 473–476.

Marr, D. (1969). A theory of cerebellar cortex. J. Physiol. *202*, 437–470.

Misgeld, U., Deisz, R.A., Dodt, H.U., and Lux, H.D. (1986). The role of chloride transport in postsynaptic inhibition of hippocampal neurons. Science *232*, 1413–1415.

Nicholson, P., and Phillips, J.M. (1981). Ion diffusion modified by tortuosity and volume fraction in the extracellular microenvironment of the rat cerebellum. J. Physiol. *321*, 225–257.

Nusser, Z., Roberts, J.D.B., Baude, A., Richards, J.G., and Somogyi, P. (1995). Relative densities of synaptic and extrasynaptic $GABA_A$ receptors on cerebellar granule cells as determined by a quantitative immunogold method. J. Neurosci. *15*, 2948–2960.

Nusser, Z., Sieghart, W., Stephenson, F.A., and Somogyi, P. (1996). The α_6 subunit of the $GABA_A$ receptor is concentrated in both inhibitory and excitatory synapses on cerebellar granule cells. J Neurosci. *16*, 103–114.

Nusser, Z., Sieghart, W., and Somogyi, P. (1998). Segregation of different $GABA_A$ receptors to synaptic and extrasynaptic membranes of cerebellar granule cells. J. Neurosci. *18*, 1693–1703.

Otis, T.S., and Mody, I. (1992). Modulation of decay kinetics and frequency of $GABA_A$ receptor-mediated spontaneous inhibitory postsynaptic currents in hippocampal neurons. Neuroscience *49*, 13–32.

Pearce, R.A. (1993). Physiological evidence for two distinct $GABA_A$ responses in rat hippocampus. Neuron *10*, 189–200.

Persohn, E., Malherbe, P., and Richards. J.G. (1992). Comparative molecular neuroanatomy of cloned $GABA_A$ receptor subunits in the rat CNS. J Comp Neurol. *326*, 193–216.

Puia, G., Costa, E., and Vicini, S. (1994). Functional diversity of GABA-activated Cl^- currents in Purkinje versus granule neurons in rat cerebellar slices. Neuron *12*, 117–126.

Quirk, K., Gillard, N.P., Ragan, C.I., Whiting, P.J., and McKernan, R.M. (1994). Model of subunit composition of γ-aminobutyric acid A receptor subtypes expressed in rat cerebellum with respect to their α and γ/δ subunits. J. Biol. Chem. *269*, 16020–16028.

Rossi, D.J., and Slater, N.T. (1993). The developmental onset of NMDA receptor-channel activity during neuronal migration. Neuropharmacology *32*, 1239–1248.

Salin, P.A., and Prince, D.A. (1996). Spontaneous $GABA_A$ receptor-mediated inhibitory currents in adult rat somatosensory cortex. J. Neurophysiol. *75*, 1573–1588.

Saxena, N.C., and MacDonald, R.L. (1996). Properties of putative cerebellar γ-aminobutyric $acid_A$ receptor isoforms. Mol. Pharmacol. *49*, 567–579.

Silver, R.A., Traynelis, S.F., and Cull-Candy, S.G. (1992). Rapid-time-course miniature and evoked excitatory currents at cerebellar synapses in situ. Nature *355*, 163–166.

Silver, R.A., Cull-Candy, S.G., and Takahashi, T. (1996). Non-NMDA glutamate receptor occupancy and open probability at a rat cerebellar synapse with single and multiple release sites. J. Physiol. *494*, 231–250.

Solis, J.M., and Nicoll, R.A. (1992). Postsynaptic action of endogenous GABA released by nipecotic acid in the hippocampus. Neurosci. Lett. *147*, 16–20.

Stevens, C.F., and Wang, Y. (1994). Changes in reliability of synaptic function as a mechanism for plasticity. Nature *371*, 704–707.

Takahashi, M., Billups, B., Rossi, D., Sarantis, M., Hamann, M., and Attwell, D. (1997). The role of glutamate transporters in glutamate homeostasis in the brain. J. Exp. Biol. *200*, 401–409.

Thompson, S.M., and Gähwiler, B.H. (1992) Effects of the GABA uptake inhibitor tiagabine on inhibitory synaptic potentials in rat hippocampal slice cultures. J. Neurophysiol. *67*, 1698–1701.

Tia, S., Wang, J.F., Kotchabhakdi, N., and Vicini, S. (1996a). Developmental changes of inhibitory synpatic currents in cerebellar granule neurons: role of $GABA_A$ receptor alpha 6 subunit. J. Neurosci. *16*, 3630–3640.

Tia, S., Wang, J.F., Kotchabhakdi, N., and Vicini, S. (1996b). Distinct deactivation and desensitization kinetics of recombinant $GABA_A$ receptors. Neuropharmacology *35*, 1375–1382.

Tyrrell, T., and Willshaw, D. (1992) Cerebellar cortex: its simulation and the relevance of Marr's theory. Philos. Trans. R. Soc. Lond. *336*, 239–257.

Varecka, L., Wu, C.-H., Rotter, A., and Frostholm, A. (1994). $GABA_A$/benzodiazepine receptor α_6 subunit mRNA in granule cells of the cerebellar cortex and cochlear nuclei: expression in developing and mutant mice. J. Comp. Neurol. *339*, 341–352.

Vincent, P., Armstrong, C.M., and Marty, A. (1992). Inhibitory synaptic currents in rat cerebellar Purkinje cells: modulation by postsynaptic depolarization. J. Physiol. *456*, 453–471.

Wall, M.J., and Usowicz, M.M. (1996). Postnatal development of spontaneous GABAergic transmission at the Golgi cell-granule cell synapse of rat cerebellum. J. Physiol. *494*, 83P.

Wall, M.J., and Usowicz, M.M. (1997). Development of action potential-dependent and independent spontaneous $GABA_A$ receptor-mediated currents in granule cells of postnatal rat cerebellum. Eur. J. Neurosci. *9*, 533–548.

Wisden, W., Korpi, E.R., and Bahn, S. (1996). The cerebellum: a model system for studying $GABA_A$ receptor diversity. Neuropharmacology *35*, 1139–1160.

Zheng, T., Santi, M.-R., Bovolin, P., Marlier, L.N.J.-L., and Grayson, D.R. (1993). Developmental expression of the α_6 $GABA_A$ receptor subunit mRNA occurs only after cerebellar granule cell migration. Dev. Brain Res. *75*, 91–103.

Zhou, Z., Misler, S., and Chow, R.H. (1996). Rapid fluctuations in transmitter release from single vesicles in bovine adrenal chromaffin cells. Biophys. J. *70*, 1543–1552.

Zhu, W.J., Wang, J.F., Krueger, K.E., and Vicini, S. (1996). δ subunit inhibits neurosteroid modulation of $GABA_A$ receptors. J. Neurosci. *16*, 6648–6656.